



# Uniformity index measurement technology using thermocouples to improve performance in urea-selective catalytic reduction systems

Sangki Park<sup>1</sup> · Jungmo Oh<sup>2</sup>

Received: 22 November 2017 / Accepted: 28 April 2018 / Published online: 4 May 2018  
© Springer-Verlag GmbH Germany, part of Springer Nature 2018

## Abstract

The current commonly used nitrogen oxides ( $\text{NO}_x$ ) emission reduction techniques employ hydrocarbons (HCs), urea solutions, and exhaust gas emissions as the reductants. Two of the primary denitrification  $\text{NO}_x$  ( $\text{DeNO}_x$ ) catalyst systems are the HC-lean  $\text{NO}_x$  trap (HC-LNT) catalyst and urea-selective catalytic reduction (urea-SCR) catalyst. The secondary injection method depends on the type of injector, injection pressure, atomization, and spraying technique. In addition, the catalyst reaction efficiency is directly affected by the distribution of injectors; hence, the uniformity index (UI) of the reductant is very important and is the basis for system optimization. The UI of the reductant is an indicator of the  $\text{NO}_x$  conversion efficiency (NCE), and good UI values can reduce the need for a catalyst. Therefore, improving the UI can reduce the cost of producing a catalytic converter, which are expensive due to the high prices of the precious metals contained therein. Accordingly, measurement of the UI is an important process in the development of catalytic systems. Two of the commonly used methods for measuring the reductant UI are (i) measuring the exhaust emissions at many points located upstream/downstream of the catalytic converter and (ii) acquisition of a reductant distribution image on a section of the exhaust pipe upstream of the catalytic converter. The purpose of this study is to develop a system and measurement algorithms to measure the exothermic response distribution in the exhaust gas as the reductant passes through the catalytic converter of the SCR catalyst system using a set of thermocouples downstream of the SCR catalyst. The system is used to measure the reductant UI, which is applied in real-time to the actual SCR system, and the results are compared for various types of mixtures for various engine operating conditions and mixer types in terms of NCE.

## 1 Introduction

Nitrogen oxides ( $\text{NO}_x$ ) are exhaust gases emitted from a diesel vehicle that produce photochemical smog, which can enter the human body through somatic cells, causing respiratory problems. Due to the serious social problems associated with smog, restrictions on emission regulations have intensified [1]. Accordingly, various combustion techniques have been developed and combined to adequately respond to such regulations. However, such efforts have reached a limit on deregulation, and therefore are inevitable to adopt the inevitable

technology [2–5]. The  $\text{DeNO}_x$  after-treatment technology commonly used to reduce  $\text{NO}_x$  employs HC and urea solution as the reductants and a secondary injection type catalytic converter system that sprays these reductants directly on the exhaust gas downstream of the combustion chamber [6–8]. There is a widely used  $\text{DeNO}_x$  system that includes lean  $\text{NO}_x$  trap (LNT) catalyst and selective catalytic reduction (SCR) catalyst. The LNT catalyst system is commonly used for the HC-LNT system, which uses hydrocarbon (HC) as the reductant. Since the HC-LNT system utilizes fuel, there is no need for an additional fuel. Therefore, the HC-LNT system can be used for engines smaller than 2.5 l. HC-LNT systems involve the unavoidable disadvantage of low fuel efficiency, so efforts have been made to maximize fuel efficiency [9, 10]. In contrast, the urea-SCR system that utilizes a urea solution as the reductant is commonly used for SCR catalyst systems [11]. The urea-SCR system features high  $\text{NO}_x$  conversion efficiency (NCE), but a separate urea solution tank is required for each vehicle. Therefore, this technique is used for vehicles equipped with relatively large engines (more than 3.0 l). In

✉ Jungmo Oh  
jmoh@mmu.ac.kr

<sup>1</sup> Transportation Pollution Research Center, National Institute of Environmental Research, Incheon 22689, Republic of Korea

<sup>2</sup> Division of Marine Engineering, Mokpo National Maritime University, Mokpo-si, Jeollanam-do 58628, Republic of Korea

general, an additional catalyst is needed to remove ammonia ( $\text{NH}_3$ ); this is because  $\text{NH}_3$  slip can be harmful to humans, and research to minimize the amount of  $\text{NH}_3$  slip is in progress [12–19].

As mentioned above, the NCEs of the HC-LNT system and the urea-SCR system, which require secondary injection, will vary depending on the type of injection system or the type of injector, injection pressure, atomization, and spray technology. Therefore, a secondary injector mounted on the exhaust pipe upstream of the catalytic converter is best suited for controlling the exhaust gas supply. Since the distribution of the injected reductant from the catalytic converter system to the catalytic converter directly influences the efficiency of the catalytic reaction, the uniformity index (UI) of the reductant distribution is the basis for system optimization. The UI for high reductant rates is an outstanding indicator of the NCE. Therefore, finding the necessary amount of catalyst can help reduce the required capacity. This can significantly reduce the manufacturing cost by reducing the amount of precious metals required for the catalytic converter. In addition, the UI of the reductants can be utilized to optimize the system components such as the reductant injection system, exhaust pipe layout, catalyst location, and arrangement. Therefore, measuring the UI is considered an important process during system development [15–17].

There are two commonly used methods for measuring the reductant UI: (i) measuring the emissions at each measuring point in the catalytic converter both upstream/downstream and (ii) acquiring reductant distribution images in the exhaust pipe upstream of the catalytic converter. Although these previously researched methods are the most reliable, they involve repeated tests at the same test conditions to obtain the results for one experimental condition. This process is not advantageous for several reasons, including the cost of engine operation, the time spent to repeat the same experiment, the multiple tasks involved (including graphing the results and compensating for disturbances in the exhaust gas flows due to the measuring probe), the high price of the equipment used to measure the exhaust emissions, and the maintenance costs [20, 21].

Measurement of the droplet uniformity index (DUI) in the exhaust pipe section of the catalytic converter section was introduced in a previous study [22, 23]. This is preferable to measurements using high-speed cameras upstream of the catalytic converter. The high-speed camera method has the advantages of bypassing the reductant distribution upstream of the catalytic converter and ensuring visual observation. However, since the section upstream of the catalytic converter is visualized without a catalytic converter, the effects of the catalytic converter installation are unknown, and the requirements for maintaining a proper back-pressure cannot be determined. Therefore, the correct flow rate and distribution cannot be measured after combination of the reductant and exhaust gas in the exhaust pipe.

The reductants are injected over the exhaust pipe that contains the high-temperature exhaust gases, resulting in

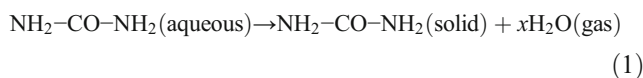
evaporation of the reductants. The reductant evaporation results in a decrease in the local temperature, and the evaporated reductant travels through the catalytic converter and converts the  $\text{NO}_x$  in a chemical reaction. Therefore, the reductant distribution UI can be estimated by measuring the temperature distribution upstream of the LNT catalyst system or the SCR De $\text{NO}_x$  catalytic converter system. In addition, when the reductant of the SCR De $\text{NO}_x$  catalytic converter system is excessively active, an exothermic reaction occurs at approximately 20 °C when passing through the catalytic converter. In this case, the local excess concentration differs from the temperature distribution and the reductant distribution, and it may be possible to measure UI in real-time by measuring the temperature increase.

The purpose of this study was to develop systems and algorithms to measure the emission of exhaust gases using thermocouples for thermo uniformity index (TUI) in the urea-SCR system, through which the reductant distribution or UI can be measured in real-time. Various experiments were conducted to minimize wall-wetting, which is a problem in catalytic efficiency. Then, the correlation of temperature was derived. The results of the measurements were compared in terms of NCE for the various types of mixers used in the actual SCR system.

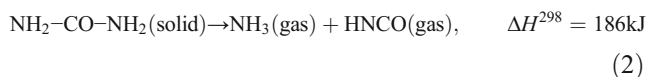
## 2 Experimental apparatus and procedures

### 2.1 Reactions of the SCR

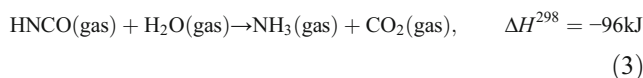
The water-soluble urea used in the SCR system for vehicles is composed of 32.5 wt% urea and 67.5 wt% water. When the urea solution is injected onto the hot exhaust gas flow upstream of the SCR catalytic, the urea solution starts to hydrolyze and to generate  $\text{NH}_3$  at 160 °C or higher through the following three steps [24]. Urea is usually applied in urea-SCR as an aqueous solution. If this solution is atomized into the hot exhaust gas stream the first step is the evaporation of water from the droplets:



Pure urea will then heat up and decompose thermally according to:



Equimolar amounts of ammonia and isocyanic acid are thus formed. Isocyanic acid is very stable in the gas phase, but hydrolyzes easily on many solid oxides with water vapor originating from the combustion process:

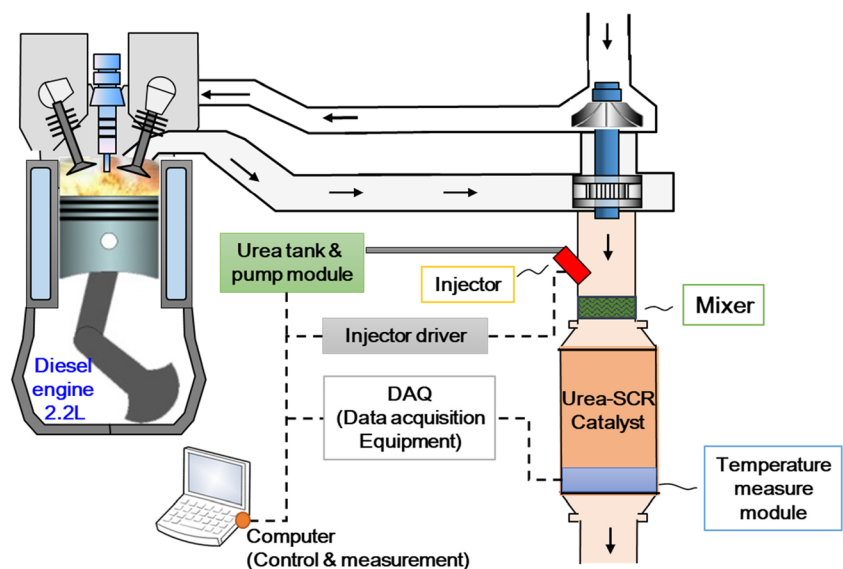


Among the SCR catalyst reactions noted above, Eq. (1) and Eq. (2) are related to the evaporation upstream of the exhaust gas inflow of the catalytic converter, which may cause heat absorption from exhaust gases. In the case of Eq. (3), an exothermic reaction may occur within the SCR catalyst. Therefore, the heat distribution upstream/downstream of the catalyst may be measured during the endothermic and exothermic reactions; therefore, the sectional distribution or UI can be properly measured.

## 2.2 Urea-SCR system with the temperature measurement module

Figure 1 shows the diesel engine exhaust system with the temperature measurement module. The urea-SCR catalyst system was installed downstream of the engine exhaust manifold and upstream of the catalyst to reduce the  $\text{NO}_x$ . The urea solution is supplied from the urea tank and pump module to the injector at the exhaust manifold. The injection quantity of the urea solution is relayed to the injector operating driver based on a pulse width modulation (PWM) signal provided by the computer. The injector pulse width and duty ratio can be controlled using this computer-based approach. The urea solution is evaporated, travels through the SCR catalyst, and then enters the temperature measurement module that was developed in this study and installed downstream. The exhaust gas temperature fluctuation is measured at each point. The temperature data are delivered from the data acquisition system (DAQ) connected to the temperature measurement module to the computer in real-time. The local temperature increase after the exothermic reaction due to the SCR catalyst is measured by means of the measurement program developed in this study to measure the temperature distribution and UI.

**Fig. 1** System layout of the urea-SCR catalyst and the thermo-measure module with the engine

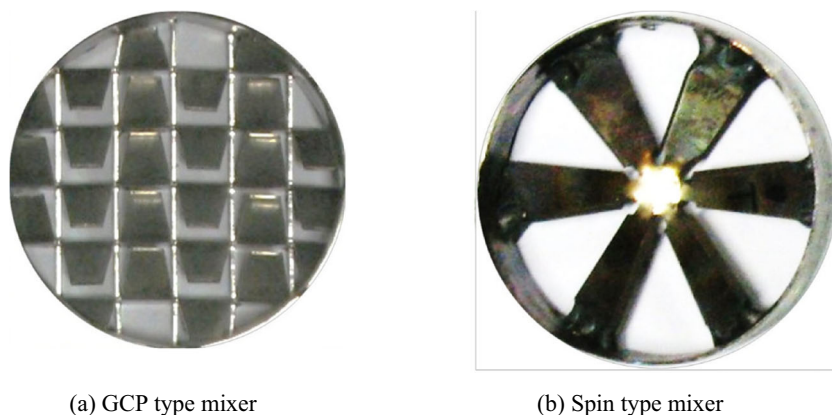


As shown in Fig. 1, the injector, which is attached at a certain angle to the wall of the straight exhaust pipe, requires a mixer. This mixer prevents wall-wetting (which prevents urea deposition), creates a uniform distribution of reductant droplets injected into the hot exhaust gas flows, and facilitates mixing of the urea with the exhaust gas. In previous study, when the GCP type mixer was used, the loss of reducing agent due to wall-wetting was smallest; thus, the  $\text{NO}_x$  conversion efficiency was the highest [23]. In this study, a grid channel plate-type mixer (GCP mixer) and a spin-type mixer were used in the UI comparative experiment as shown in Fig. 2.

## 2.3 The structure and design of the temperature measurement module

The temperature measurements in this study included measurements from 19 thermocouples. The measured temperature of the exhaust gas flow area was divided into measurements of the same size and can be separated by dividing the temperature measurement area at certain intervals. A 2D CAD hexagonal lattice was used for each unit area (cell) to individually measure temperatures, and a honeycomb-shaped inner frame was added to the outer frame, which had the same diameter as the catalyst downstream. 'POS.1' was identified as the unit area at the center of the measuring range, and unit areas were added on all sides. The temperature was measured at the center of each unit area. The inner frame in a stainless consisted of squares or triangles. For triangular inner frames, the distance from the periphery of adjacent units to neighboring units may differ from areas adjacent to neighboring areas. Therefore, the thermocouples in each unit were not separated or arranged at the same time in every direction. In addition, although thermocouples can be separated equally in all directions when the unit is formed, it is difficult to design the interior frame for

**Fig. 2** Photographs of the mixer types



such a case. Therefore, the internal frame was designed as a hexagonal checked structure so that the unit areas were hexagonal and the center-to-center distance of the unit areas were the same in all directions. This internal frame was easy to produce. Using the hexagonal structure for the internal frame, the external space inside the external frame can be fully utilized, and an external force can smoothly supply the exhaust gas flow, which improves the durability. The parts of the hexagonal-shaped structure formed a hexagonal grid. Figure 3 shows such a 2D CAD-based hexagonal structure and the corresponding system.

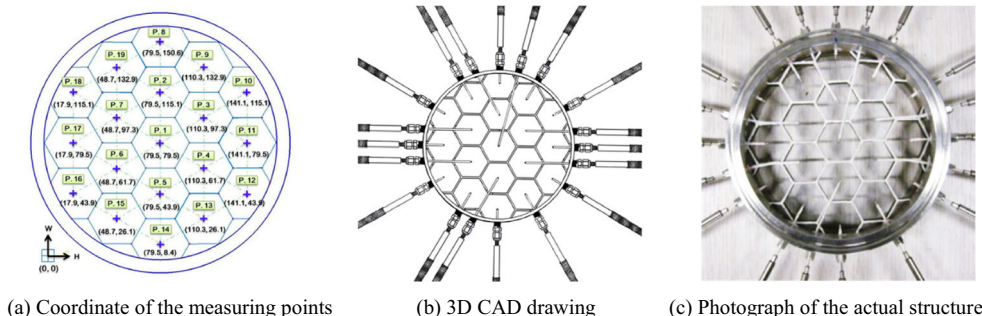
As shown in Fig. 3 (a), the location and insertion direction of each thermocouple in the 2D CAD were converted from 3D CAD as in Fig. 3 (b), and the resulting image is shown in Fig. 3 (c). The exhaust gas flow through the center of each cell was separated from the inner frame of the hexagonal image. Therefore, the effect of internal frames was minimized without influencing the internal frame design. In the area adjacent to the internal frame or the edge of the cell, however, the friction with the inner frame causes changes in the flow patterns. Therefore, to obtain measurements at the thermocouples that would be similar to the case without an internal frame, the center of each cell was chosen as the temperature measurement location. In addition, the insulator was distributed across all internal areas except for the edge or temperature sensing part of the thermocouple in order to avoid thermal conduction through the internal frame and thermocouples. The white section inside the figure represents the area covered with heat insulating ceramics.

The thermocouples used in this study were K-type-A-class 1.6 mm. The small size of the thermocouples minimizes their influence on the exhaust gas flow. Since mild temperature variations were measured at relatively high temperatures, all thermocouples were specially manufactured at the same temperature to ensure accuracy from thermocouple to thermocouple. In addition, the test results were certified in terms of the measurement uncertainty of one thermocouple, where the standard deviation was  $\pm 0.5\text{--}0.8\text{ }^\circ\text{C}$ , the level of reliability was approximately 95%, and  $k = 2$ . The results of the temperature difference between the thermocouples at the normal temperature (max.  $0.0965\text{ }^\circ\text{C}$ ) demonstrated excellent reliability.

**2.4 Temperature data acquisition and data conversion algorithm**

Temperature data were obtained using the data acquisition system (DAQ) and were passed to the computer. Temperature measurements were initiated after the input of basic data regarding sensor positions, numbers, and measurement ranges. The reductant UI is expected to be more accurate if the exhaust gas flow section is specified and the number of thermocouples in the unit is large. However, excessive increases in the size of the internal frame to accommodate an increased number of thermocouples resulted in flow failure in the exhaust gas. As a result, the accuracy of the reductant UI was decreased.

**Fig. 3** Coordinates of the measurement points of the thermo-measure module



In this study, the urea section was 159 mm, and it was divided into 19 cells with a thermocouple in the center of each cell. Therefore, it was necessary to expand the data provided by the thermocouples to cover the entire cross-sectional area. Interpolation was used for this purpose. In general, interpolation methods include linear interpolation, polynomial interpolation, and spline interpolation. The linear interpolation method is used to link data sets linearly, which does not guarantee accuracy. In addition, linear interpolation is disadvantageous in that it involves Runge's phenomenon, which is the serious fluctuation of the graph at the breakpoints, and this makes the values different from the actual measurements. In contrast, spline interpolation uses polynomial expressions of a low degree by dividing data sets into sections. This is different from polynomial interpolation, in which all the sections are considered one single polynomial. This process produces a relatively stable result. The algorithm developed in this study, therefore, calculates the temperature data of each unit area by means of a biharmonic spline interpolation to estimate the value of  $Z_i$  (temperature) resulting from the 2-dimensional interpolation at the point corresponding to the  $X_i/Y_i$  coordinate of each temperature sensor. The temperature values obtained through the interpolation method were applied on a grid 1 mm apart for color mapping. Using this process, the temperature distribution can be accurately measured at a temperature measurement point, and the distribution can be expressed smoothly. If the image of the catalytic converter is circular, the boundaries are truncated, and the UIs are calculated. Background zero leveling is carried out before the reductant is injected. This process was used to reset the temperature distribution to zero prior to the background zero operation. Thereafter, the injection of reductants was likely to cause a decrease in the temperature due to the latent heat of vaporization or an increase in temperature due to an exothermic reaction, which results in temperature deviation. The reductant distribution and UI can be measured based on the calculations of the color plot and UI.

Figure 4 shows both the temperature distribution downstream of the SCR catalyst prior to and after the background zero, followed by urea solution injection. The temperature

distribution of the background images shows the exhaust gas flow in the pipe at high temperatures. After equalization of the general distribution to zero, the injection of the urea solution resulted in an exothermic reaction within the SCR catalyst that increased the temperature and created the distribution. This can be regarded as the urea solution distribution. As shown in Fig. 4, the droplets of the injected urea solution may be affected by the flow field, but they are inclined to the bottom and left sides in the pipe due to the atomization distribution. The distribution of urea solution droplets can be changed in real time whenever the onsite or SCR system changes.

## 2.5 Thermo uniformity index (TUI)

The concentration UI was suggested by Weltens [25], who defined the uniformity of the flow velocity at the cross-section monolith, and then this was redefined as a UI for temperature. The defined TUI is as follows:

$$TUI = 1 - \frac{\sum_{i=1}^n |t_i - \bar{t}|}{2n \left( \bar{t} * \frac{C}{100} \right)} \quad (4)$$

Here,  $t_i$  is the local flow temperature,  $\bar{t}$  is the average temperature at the cross-section of the monolith,  $n$  is the total number of temperature data points based on interpolation within the cropped boundary, and  $C$  is the correction factor. The concentration of the element solution is uniformly distributed when the thermo uniformity index (TUI) is uniform. In this study, 19 thermocouples were used to produce the temperature data at intervals of 1 mm as shown in the color plots in Fig. 4 (b), which illustrate how the TUI was calculated.

## 2.6 Experimental procedure

The experimental apparatus shown in Fig. 1 was designed and tested to verify the applicability of the developed TUI. As shown in Table 1, the engine used for this study was a

**Fig. 4** Downstream temperature distribution

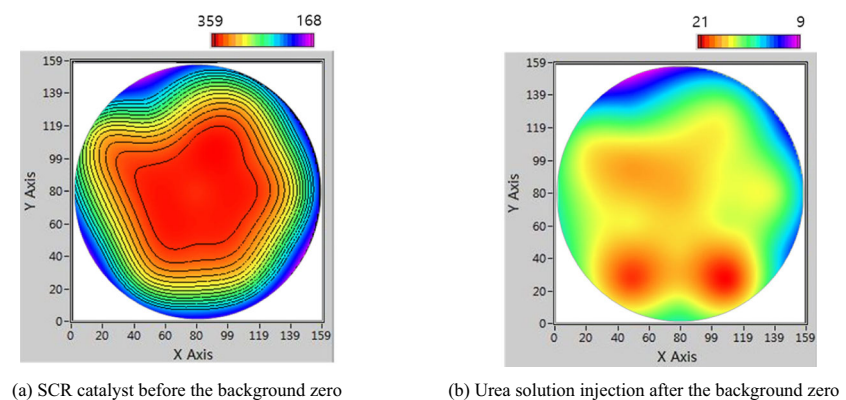


**Table 1** Specifications of the test engine

Description	Specification
Engine type	4-stroke turbo-charged DI diesel engine
Number of cylinders	In-line 4 cylinders
Bore ×stroke (mm)	85.6 × 96
Displacement volume (cc)	2199
Compression ratio	16
Fuel injection system	Common rail (Piezo type)
Valve type	DOHC valves per cylinder
Turbocharger type	Electrical variable geometry turbo charger (e-VGT)
Max. power (ps / rpm)	200 / 3800
Max. torque (Nm / rpm)	436.4 / 2000

2199 cm<sup>3</sup>, 4-cylinder diesel engine with four valves per cylinder, a common rail direct fuel injector (CRDI), and an electrical variable geometric turbocharger (e-VGT). The basic performance of this diesel engine was evaluated by measuring the amount of NO<sub>x</sub> emitted as a function of the brake mean effective pressure (BMEP) and revolutions per minute (RPM). The values are presented in Fig. 5. The engine operation conditions were BMEP 12, 15, and 15 bar at engine speeds of 1500, 1800, and 2000 rpm, respectively.

To compare the mixers, a GCP mixer and a spin mixer were installed at the locations shown in Fig. 1. The upside-down GCP mixer condition, where the GCP mixer was inserted against the gas flow direction, was added to the other three conditions in order to compare with experiments without a mixer and to examine the effects of the direction and arrangement of the channel wings at certain angles.

The specifications and injection conditions of the urea solution injector are shown in Table 2. This jet spray-type, three-hole prototype injector atomizes the pressurized liquid as it passes

through a hole with a small orifice. A urea solution containing 32.5% urea, which is commonly used for vehicles, was utilized in this study. The solution was injected 60 times at a pressure of 0.5 MPa at 4 Hz for 30 s and at a ratio of 25–30%. It was stabilized for more than 10 min while the engine was operated, and the injection strategy included a cycle of 15 s of injection followed by a 15 s rest period for a total of approximately 5 min. As for the injection duty, the ratio was controlled between 25 to 30% so that the amount of NH<sub>3</sub> slip remained as high as 10–20 ppm, and the attached angle of the injector was approximately 30 degrees from the central line of the straight pipe.

### 3 Results and discussion

#### 3.1 Characteristics of the exhaust gas flow rate and temperature

The temperature control of the engine exhaust temperature is sensitive to each component control condition in the engine. As shown in Table 3, the exhaust gas temperature prior to the addition of the urea solution was specified in the mixer experimental conditions. Each engine speed and load were measured downstream of the SCR catalyst, and the exhaust gas flow rate was calculated under the same conditions. At 1500 rpm and 12 bar, the temperature at the red part of the

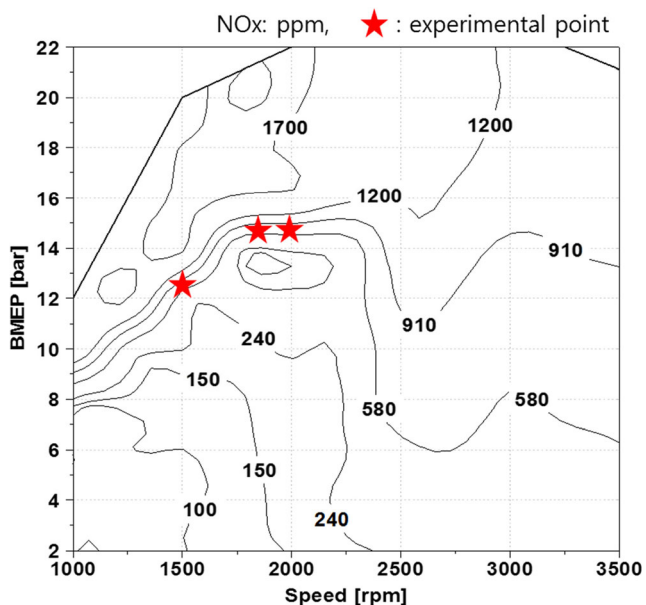


**Fig. 5** NO<sub>x</sub> emissions as a function of BMEP and RPM

**Table 2** Specifications of the urea solution injector and injection conditions

Description	Specification
Nozzle type	Jet-spray
Spray geometry	Triple stream
Urea solution	32.5%
Injection pressure	0.5 MPa
Injection frequency	4 Hz
Injection duty	25, 30%
Injection number	60
Repetition time	30s

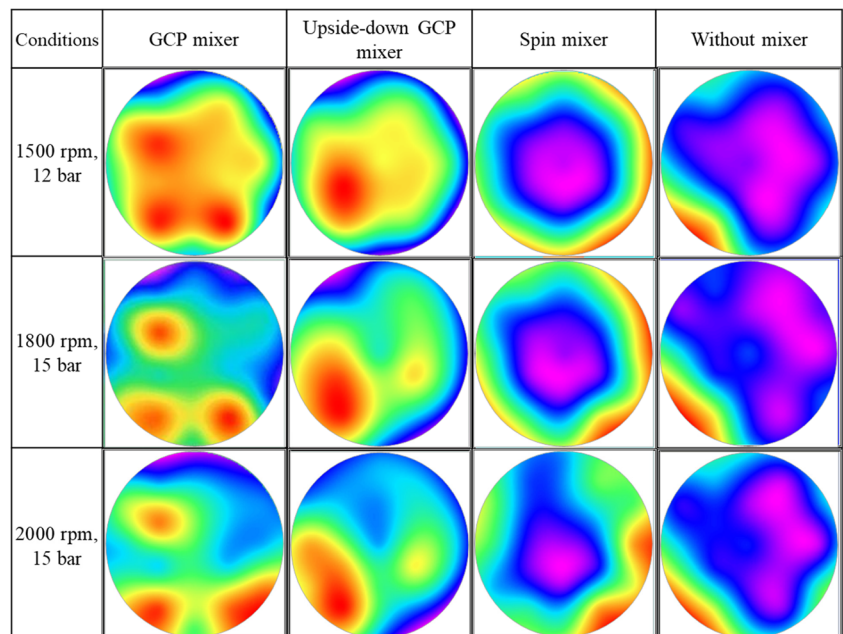
**Table 3** Exhaust gas temperatures for each set of experimental conditions

Engine speed (rpm)	BMEP (bar)	Exhaust gas flow rate (kg/h)	Exhaust gas temperature central/mean (°C)	
1500	12	130	Without mixer	379 / 311
			GCP mixer	359 / 299
			Upside-down GCP mixer	373 / 315
			Spin mixer	376 / 303
1800	15	175	Without mixer	433 / 364
			GCP mixer	430 / 362
			Upside-down GCP mixer	437 / 379
			Spin mixer	431 / 365
2000	15	200	Without mixer	444 / 380
			GCP mixer	442 / 381
			Upside-down GCP mixer	445 / 388
			Spin mixer	438 / 375

center shown in Fig. 4 (a) was between 359 and 379 °C, and the mean temperature over the general area of the round pipe was between 299 and 315 °C. When the load changed from 12 to 15 bar, the central temperature was between 430 and 437 °C, and the mean temperature drastically increased up to 362–379 °C. In contrast, when the engine speed changed with the same load, the temperature increase was not significant, which indicates that the exhaust gas temperature is significantly affected by the load (or BMEP), and that the exhaust gas flow rate is affected by changes in the engine speed.

Figure 6 compares the exothermic temperature deflection for various mixers at different engine speeds and load conditions. When no mixer was used, the temperature distribution at seven o'clock direction was obtained. The droplets injected from the injector that was attached to the exhaust pipe at 30°

were inclined in the direction of the injection without the mixer. In contrast, when the GCP mixer was used, the temperature distribution was the most widespread of all the experimental conditions. The triple stream atomization was observed based on the injector characteristics, which resulted in minimal wall-wetting. Since wall-wetting can cause urea deposits, and this is closely linked to the catalyst efficiency [23], the GCP mixer should be most effective in terms of the distribution of the exothermic temperature deflection. The injected reductant was not widely distributed without a mixer, and the distribution was better with the GCP mixer. The spin mixer rotates the exhaust gas flow, which facilitated the distribution toward the column. As a result, the temperature at the center of the hollow sphere was relatively low, while most of the droplets were concentrated in the direction of the column.

**Fig. 6** Comparison of the exothermic temperature deflection for each condition

### 3.2 Comparison of the NCE and TUI without a mixer

Figure 7 shows the results of a comparison of the  $\text{NO}_x$  emissions, TUI, and NCE as a function of the engine speed and load when no mixer was installed. With no mixer, the NCE was high during the initial injection, which resulted from the active evaporation of the urea solution within the pipe after wall-wetting, as shown in Fig. 6. After the second injection, the NCE was lower than in the initial stage. When 1500 rpm was reached, the NCE changed based on the injection pattern instead of remaining high. Although the urea solution injection was insufficient, and this clearly had an effect, a 30% increase in the injection duty did not change the TUI or NCE significantly, while the  $\text{NH}_3$  slip increased. This result is because reductant was lost through wall-wetting, and this lost reductant was supposed to help decrease the TUI and NCE. However, some of the reductant was not fully activated. In general, the extent of the changes in the TUI and NCE were similar to one other. Wave-like behavior was observed in the data at similar intervals, which is more evident under other experimental conditions. Therefore, we concluded that the TUI measurement method could be compared with the NCE results.

As the engine speed increased, the NCE decreased and the TUI increased to some extent. This result was because

reductant concentration was insufficient or the exothermic reaction was insignificant in most areas based on the function used for the TUI calculation.

### 3.3 Comparison of the NCE and TUI based on the mixer type

When a GCP mixer was used, the NCE gradually increased as urea injection continued. The TUI and NCE remained at a high level up to 85% or higher even though the engine speed or exhaust gas flow rate changed. As shown in Fig. 6, the wall-wetting remained minimal even at a high engine speed, and the exothermic temperature deflection and urea solution droplets were widely distributed.

In contrast, the TUI and NCE for the upside-down GCP mixer (as explained earlier) were generally lower than those of the regular GCP mixer installation. The same injection duty was executed at an engine speed of 1500 rpm. Since the  $\text{NH}_3$  slip increased when the same injection duty was used at 1800 rpm, the injection duty was set to 25%. Therefore, the TUI and NCE decreased when the injection quantity of the urea solution was insufficient because more wall-wetting occurred in the upside-down GCP mixer case than in the regular GCP mixer case as shown in Figs. 8 and 9. At an

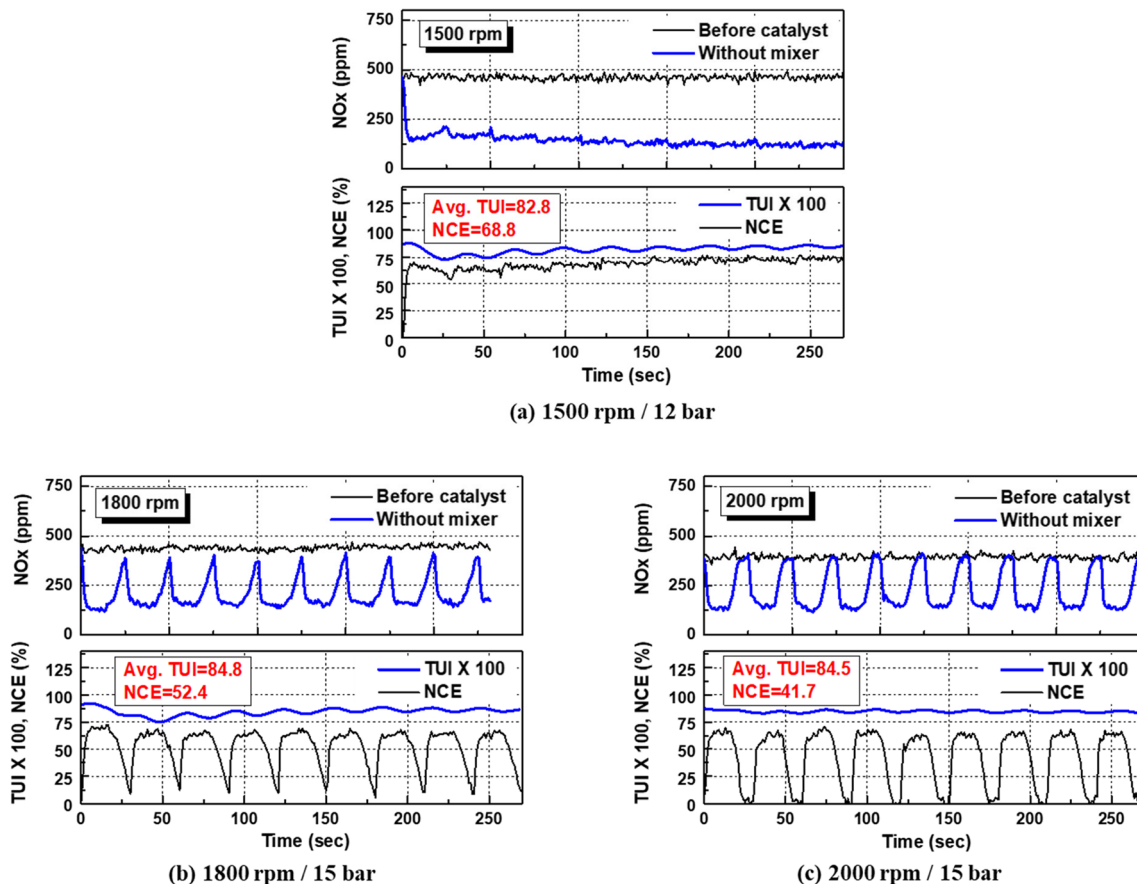
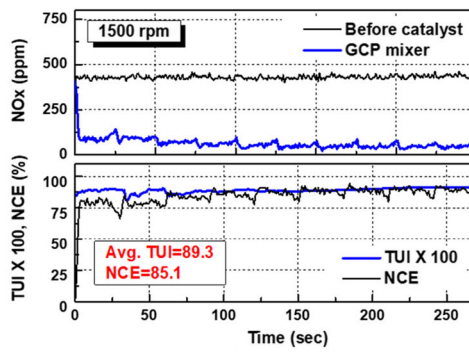
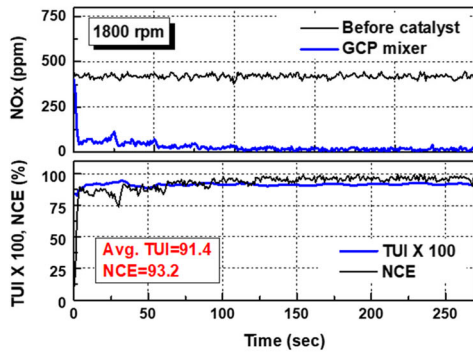


Fig. 7 TUI and NCE for various engine speeds and loads without a mixer

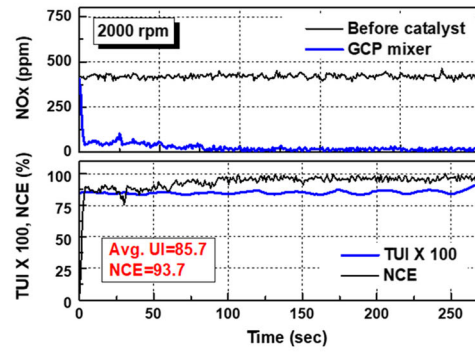




(a) 1500 rpm / 12 bar

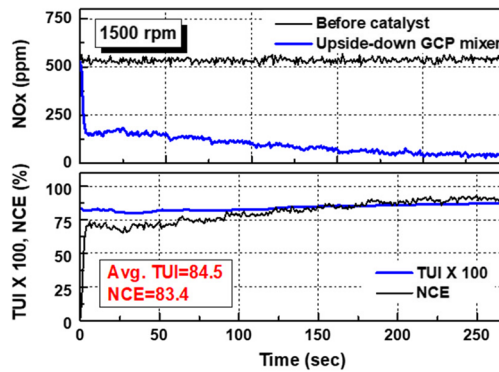


(b) 1800 rpm / 15 bar

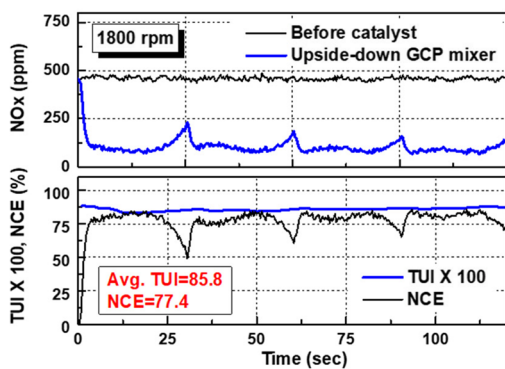


(c) 2000 rpm / 15 bar

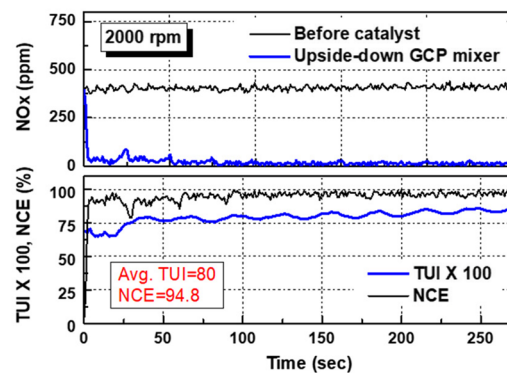
Fig. 8 TUI and NCE for various engine speeds and loads with a GCP mixer



(a) 1500 rpm / 12 bar



(b) 1800 rpm / 15 bar



(c) 2000 rpm / 15 bar

Fig. 9 TUI and NCE for various engine speeds and loads with an upside-down GCP mixer

engine speed of 2000 rpm, however, the NCE increased when the TUI decreased. One may have expected that wall-wetting would increase based on the results shown in Fig. 6, but evaporation of some of the droplets was facilitated due to wall-wetting.

The direction of the GCP mixer installation was reversed to compare the effects of orientation and arrangement of the channel wings on the reflection of the structural characteristics of a GCP mixer. The standard installation was found to be more effective. These results illustrate that it is vital to optimize the structure of the mixer to obtain an appropriate injection angle, atomization shape, and pattern for the urea solution [23].

When a spin mixer was used, no significant changes were observed as the engine speed changed since the temperature of the hollow sphere shape of the TUI generally remained low. The NCE remained high during the initial injection period for all engine speeds because the evaporation of the urea solution droplets was facilitated by the wall-wetting within the heated pipe prior to the urea solution injection. At a low engine speed or low exhaust gas flow rate, the NCE remained high, and low wall-wetting was expected as shown in Fig. 10. In contrast, as the engine speed increased, the level gradually decreased. This is because urea solution wall-wetting occurred as the exhaust gas flow rate increased within the pipe due to the rotational force. Therefore, the efficiency of a spin mixer is expected to

be better under low engine speed and low exhaust gas flow rate conditions where the liquid flows are not significantly affected.

Figure 11 shows a graph that summarizes the results of the TUI and NCE for various mixers at engine speeds of 1500, 1800, and 2000 rpm. In general, the TUI remained abnormally high, but the lowest NCE was observed when no mixer was used due to wall-wetting. As the engine speed changed, the NCE fluctuated more significantly (TUI: 0.83–0.85, NCE: 42–69%). In contrast, when a spin mixer was installed, the values of the TUI and NCE were a bit higher, and the fluctuation rate of the NCE was accordingly higher (TUI: 0.83–0.9, NCE: 58–92%). In the case of the upside-down GCP mixer, the fluctuation rate was higher than that of the standard GCP mixer (TUI: 0.8–0.86, NCE: 77–95%). When a GCP mixer was used, the TUI and NCE were stable and changed the least as the engine speed changed; in addition, the TUI and NCE remained high (TUI: 0.86–0.91, NCE: 85–94%). Therefore, we concluded that a GCP mixer is the most appropriate mixer for general engine operation conditions. The upside-down GCP mixer and the spin mixer (in that order) were found to be more effective than an installation without a mixer. This result shows that a mixer is an essential element when an injector is attached to the wall of the straight exhaust pipe at a certain angle.

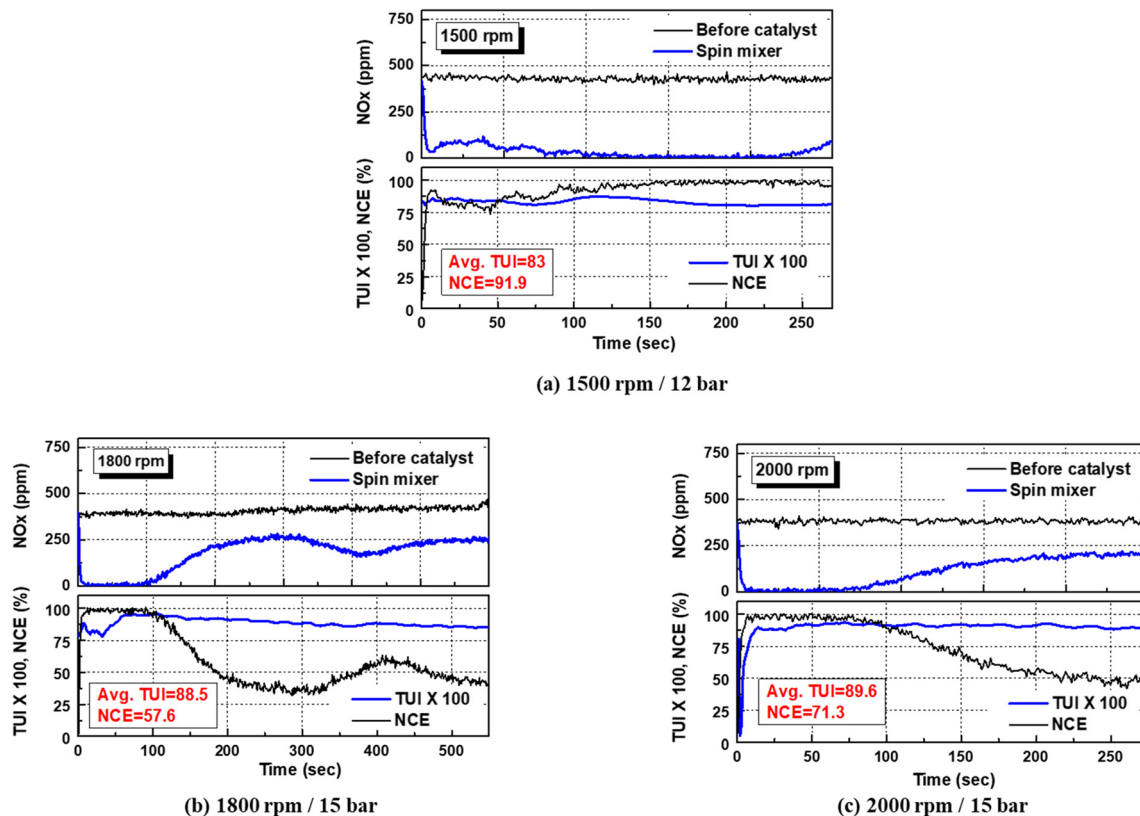


Fig. 10 TUI and NCE for various engine speeds and loads using a spin mixer

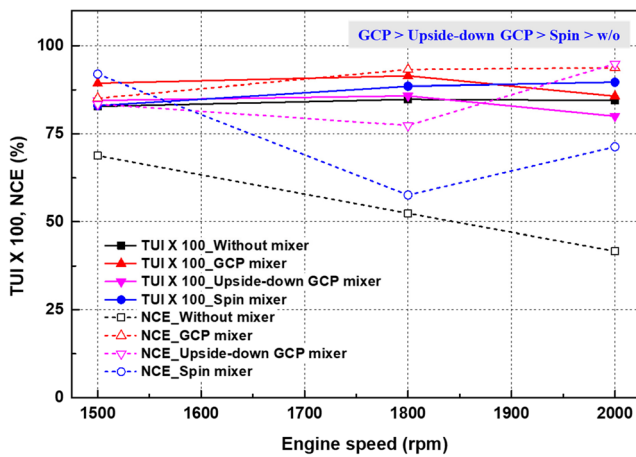


Fig. 11 Comparison of the TUI and NCE for various mixer types at different engine speeds

The graph in Fig. 12 shows the engine speed range over which the effects of a GCP mixer would be the most significant. The GCP mixer improved the TUI by 1.4 to 7.9% and improved the NCE by 23.7 to 124.7%. No significant difference was shown with regard to the TUI in this study because the temperature distribution of the hollow sphere shape and the wall-wetting were highly influential. As shown in Fig. 11, when wall-wetting effects are insignificant (as in the case of the GCP mixer and the upside-down GCP mixer), this can be an effective method for optimizing a system in terms of the temperature deflection, distribution, and TUI.

## 4 Conclusions

A method of measuring UI for the urea-SCR system was developed using thermocouples to measure the TUI under different engine operation conditions using different types of mixers. The characteristics and effects of each mixer were compared based on the NCE, and we reached the following conclusions:

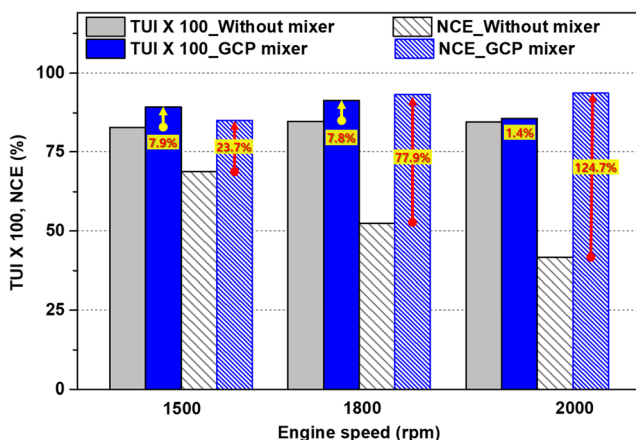


Fig. 12 Effects of the GCP mixer on the TUI and NCE for various engine speeds

- (1) The distribution of the exothermic temperature deflection was measured for various mixers. The use of a GCP mixer provided a wide distribution in comparison to other mixer conditions. The experimental results also clearly showed that atomization was of the triple stream type, and that a GCP mixer was the most effective since it involved the least wall-wetting.
- (2) The exothermic temperature deflection results showed that wall-wetting hindered the reductants from being sufficiently activated, caused a loss of reductants, and decreased the TUI and NCE.
- (3) Since the GCP mixer involved the least wall-wetting at a high engine speed and facilitated the wide distribution of urea solution droplets based on the exothermic temperature deflection, the TUI and NCE remained at a high level (up to 85% or higher). In addition, a spin mixer proved to be effective at a low engine speed and low exhaust gas flow rate since the effects of the exhaust gas flows would be insignificant.
- (4) The values of the TUI and NCE were as follows: no mixer, TUI = 0.83–0.85 and NCE = 42–69%; with a spin mixer, TUI = 0.83–0.9 and NCE = 58–92%; with an upside-down GCP mixer, TUI = 0.8–0.86, NCE = 77–95%. When a GCP mixer was installed, the TUI and NCE were stable and fluctuated less during changes in the engine speed. The values of TUI and NCE also remained high, up to TUI = 0.86–0.91 and NCE = 85–94%.
- (5) We concluded that a GCP mixer would be the most appropriate to establish engine operation conditions. A mixer is an essential element when an injector is attached to the wall of the straight exhaust pipe at a certain angle.

**Acknowledgements** This research was supported by Basic Science Research Program through the National Research Foundation of Korea (NRF) funded by the Ministry of Education. (No. NRF-2015R1D1A3A01019661).

**Publisher's Note** Springer Nature remains neutral with regard to jurisdictional claims in published maps and institutional affiliations.

## References

1. Luo Z, Hu S, Chen D, Zhu B (2018) From production to consumption: a coupled human–environmental nitrogen flow analysis in China. *Environ Sci Technol* 52:2025–2035
2. Prabhu S, Nayak N, Kapilan N, Hindasageri V (2017) An experimental and numerical study on effects of exhaust gas temperature and flow rate on deposit formation in urea-selective catalytic reduction (SCR) system of modern automobiles. *Appl Therm Eng* 111: 1211–1231
3. Guan B, Zhan R, Lin H, Huang Z (2014) Review of state of the art technologies of selective catalytic reduction of NO<sub>x</sub> from diesel engine exhaust. *Appl Therm Eng* 66:395–414

4. Adachi T, Aoyagi Y, Kobayashi M, Murayama T, Noda A, Goto Y, Suzuki H (2009) Effective NO<sub>x</sub> Reduction in High Boost, Wide Range and High EGR Rate in a Heavy Duty Diesel Engine. SAE Technical paper 2009–01-1438
5. Kim Y, Kim K, Lee K (2011) Effect of a 2-stage injection strategy on the combustion and flame characteristics in a PCCI engine. *Int J Automot Technol* 12:639–644
6. Johnson T (2011) Diesel Emissions in Review. *SAE Int J Engines* 4:143–157
7. Oh J, Lee K, Jeong H (2008) Study on the spray behavior and diesel fuel distribution characteristics of a secondary injector for a lean NO<sub>x</sub> trap catalyst. *Energy Fuel* 22:1527–1534
8. Forzatti P, Lietti L, Nova I, Tronconi E (2010) Diesel NO<sub>x</sub> aftertreatment catalytic technologies: analogies in LNT and SCR catalytic chemistry. *Catal Today* 151:202–211
9. Lindholm A, Currier N, Fridell E, Yezerets A, Olsson L (2007) NO<sub>x</sub> storage and reduction over Pt based catalysts with hydrogen as the reducing agent: influence of H<sub>2</sub>O and CO<sub>2</sub>. *Appl Catal B Environ* 75:78–87
10. Oh J, Lee K, Lee J (2008) A study on the optimal injection conditions for an HC-LNT catalyst system with a 12-hole type injector. *J Therm Sci Technol* 3:278–291
11. Sharma S, Fadnavis J, Khot A (2018) Empirical model to predict melt volume for different range of diesel exhaust fluid tank volumes used in selective catalytic reduction systems. *Appl Therm Eng* 129: 916–926
12. Baleta J, Martinjak M, Vujanovic M, Pachler K, Wang J, Duic N (2017) Numerical analysis of ammonia homogenization for selective catalytic reduction application. *Journal of Environ Manag* 203: 147–1061
13. Chatterjee S, Naseri M, Li J (2017) Heavy Duty Diesel Engine Emission Control to Meet BS VI Regulations. SAE Technical paper 2017–26-0125
14. Rice M, Kramer J, Mueller-Haas K, Mueller R (2007) Innovative Substrate Technology for High Performance Heavy Duty Truck SCR Catalyst Systems. SAE Technical paper 2007–01-1577
15. Ottaviani E, Jean E, Albert H, Amon B (2009) Dual Line Exhaust Design Optimisation to Maximize SCR Catalyst Efficiency thru Improved Ammonia Distribution. SAE Technical paper 2009–01-0914
16. Stein M, Bykov V, Maas U (2017) The effect of evaporation models on urea decomposition from urea-water-solution droplets in SCR conditions. *Emission Contrl Sci Technol* 3:263–274
17. Jeong S, Lee S, Kim W (2008) Numerical study on the optimum injection of urea-water solution for SCR deNO<sub>x</sub> system of a heavy-duty diesel engine to improve deNO<sub>x</sub> performance and reduce NH<sub>3</sub> slip. *Environ Eng Sci* 25:1017–1036
18. Oesterle J, Calvo S, Damson B, Feyl G, Neumann F, Rudelt J (2008) Urea Systems in Focus-New Challenges and Solutions in the Development of Car and Commercial Vehicle Exhaust Systems. SAE Technical paper 2008–01-1186
19. Lee P, Peterson A, Lai M, Casarella M, Wu M (2010) Effects of B20 fuel and catalyst entrance section length on the performance of urea SCR in a light-duty diesel engine. SAE Technical paper 2010–01-1173
20. Joo K, Jo J, Kim C, Lee J, Kim H (2008) The study of NO<sub>x</sub> reduction using urea-SCR system with CPF and DOC for light duty vehicle; the diesel NO<sub>x</sub> reduction system. SAE Technical paper 2008–01-1183
21. Zheng G, Gardner T, Kotrba A, Golin M, Majewski P (2011) Development of urea SCR systems for large diesel engines. SAE Technical paper 2011–01-2204
22. Oh J, Kim K, Lee K (2012) Spray characteristics of four-hole injectors used for a hydrocarbon lean nitrogen oxide catalyst system in a diesel engine. *Proc Instit Mech Eng Part D: J Auto Eng* 226: 1073–1087
23. Oh J, Kim K, Lee K (2012) Effects of various mixer types on the spatial distribution of a De-NO<sub>x</sub> reductant. *Fuel* 94:93–101
24. Koebel M, Elsener M, Kleemann M (2000) Urea-SCR: a promising technique to reduce NO<sub>x</sub> emissions from automotive diesel engines. *Catal Today* 59:335–345
25. Weltens H, Bressler H, Terres F, Neumaier H, Rammoser D (1993) Optimisation of catalytic converter gas flow distribution by CFD prediction. SAE Technical paper 930780